Controlling Diffusion and Exchange in Layer-by-Layer Assemblies

Nicole S. Zacharia,[†] Dean M. DeLongchamp,*[,‡] Miguel Modestino,[§] and Paula T. Hammond*[,§]

Department of Materials Science and Engineering, Massachusetts Institute of Technology, Cambridge, Massachusetts 02139; Polymers Division, National Institute of Standards and Technology, Gaithersburg, Maryland 20899; and Department of Chemical Engineering, Massachusetts Institute of Technology, Cambridge, Massachusetts 02139

Received May 12, 2006; Revised Manuscript Received December 14, 2006

ABSTRACT: Here we present a layer-by-layer (LbL) assembled device architecture that serves as a model heterostructure to study the atypical assembly that can result from the bottom-up combination of multiple multilayers of different compositions. Heterostructure assembly is disrupted by diffusion of linear poly(ethylene imine) (LPEI) within an LPEI/poly(acrylic acid) (PAA) polyelectrolyte multilayer and the exchange of LPEI with an aromatic polycation (poly(hexyl viologen) or PXV) that was assembled with PAA in an underlying multilayer. We illustrate this diffusion/exchange mechanism by showing that the assembly of an LPEI/PAA multilayer on to a PXV/PAA multilayer causes the heterostructure film to roughen and become opaque, indicating significant morphological changes. FTIR analysis confirms that LPEI diffuses into the underlying polyelectrolyte multilayer and displaces PXV. Exchange experiments of the constructed PXV/PAA multilayers in the presence of LPEI solutions were completed. Molecular weight dependence on the rate of exchange is shown through the use of high molecular weight LPEI, which is shown to undergo displacement at rates much slower than the time frame of the typical layer adsorption cycle. Finally, we prevent LPEI diffusion by incorporating a thin blocking layer of cross-linked LbL film, resulting in a discrete, compartmentalized multilayer structure. We explain these phenomena by the strength of acid−base interactions between LPEI and PAA, the ability of hydrophilic LPEI molecules to move through a multilayer, and the tendency of weak polyelectrolytes to redistribute their ionization in response to changes in immediate environment. The success of assembling a heterostructured LbL film can be predicted by whether or not the individual component layers grow superlinearly in isolation. Our system provides a model example of LbL assemblies in which interdiffusion destabilizes film growth, and by understanding the mechanism of this destabilization, we are able to control it.

Introduction

The layer-by-layer (LbL) sequential adsorption of polyelectrolytes is a promising method to reproducibly create defect-free conformal coatings.[1] The potential applications of these LbL assembled films range from drug delivery and cell resistant coatings to antireflection coatings, batteries, and electrochromic devices.[2] Advanced applications require the bottom-up assembly of complex heterostructured LbL assemblies, where a film is composed of layers of different polyelectrolyte pairs that can form various functional components of a device. Recently, we have found that the bottom-up assembly of complex heterostructures often yields unexpected results because individually assembled polyelectrolyte pairs can behave differently during heterostructure assembly than when constructed as isolated structures. Such disrupted heterostructure assemblies are caused by complex interactions between polyelectrolyte pairs, which are governed by the ionization density and distribution along the polyelectrolyte backbone.[3−5,15,26,29] Studies of the layer-by-layer process have recently revealed that in such cases the system can no longer be treated as a kinetically frozen matrix with a fixed charged surface; instead, the polyelectrolyte complex can be considered to be a dynamic network of chains in which ionic bonds can be formed or displaced throughout the thickness of the film. Gaining a greater understanding of and control over the inner structure of these assemblies is very important if one is to ultimately control and construct novel heterostructures from these systems.[8]

Typical LbL films exhibit linear growth; after the first few layer pairs, each subsequent layer pair thickness reaches a steady-state value. Recently, systems growing in a superlinear fashion have been observed.[10−13] In electrostatically bound films, exponential growth has been observed in films that are assembled from partially solvated polymers,[10] systems with strong hydrogen bonding,[11] or in systems of biological polymers.[12] It has been suggested that in certain cases nonlinear growth results from the increasing fractal roughness of the film surface, creating more film surface area with each adsorption step.[30,32] In other cases, direct evidence shows that interdiffusion of polyions within the LbL film cause superlinear growth.[15] In these cases, the depositing polymer not only adsorbs onto the film's surface but also enters the bulk of the film, creating a "reservoir" of excess unpaired polyelectrolyte. At the next step of film assembly, the contents of this reservoir are attracted to the now oppositely charged surface, polyelectrolyte is drawn out from the bulk film, and complexes with oppositely charged polyelectrolyte at the surface. As film thickness increases, the size of this reservoir increases, leading to superlinear growth. It is also possible for free polyions to exchange with polymer chains that are already a part of the bulk film.[15,16] This exchange can be a polyion either reversibly exchanging with itself or irreversibly replacing another polymer, which forms a complex that is less energetically favored.[15,33] Diffusion within an LbL assembly, while typically promoting disorder within the bulk film, can in certain instances be used to segregate and order species at the surface, as shown recently in the assembly and

* To whom correspondence should be addressed. E-mail: dean.delongchamp@nist.gov; hammond@mit.edu.
[†] Department of Materials Science and Engineering, MIT.
[‡] National Institute of Standards and Technology.
[§] Department of Chemical Engineering, MIT.

10.1021/ma061080f CCC: $37.00
Published on Web 02/08/2007

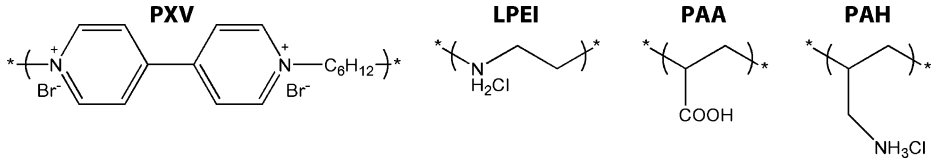

Figure 1. Polyelectrolyte primary chemical structures; the primary and secondary amines as well as the carboxylic acid are shown in their protonated (low pH) forms.

entropic ordering of viruses within an LbL assembled thin film.[16]

When interdiffusion occurs during assembly, one might expect heterostructure assembly to be disrupted when including a superlinearly growing LbL layer. Our system is composed of one polyelectrolyte pair, $(PXV/PAA)_n$, incorporating a strong polycation with a fixed ionization density and charge distribution,[10] and one pair, $(LPEI/PAA)_n$, incorporating a weak polycation with a labile ionization density and charge distribution that is dependent upon the local environment.[26,34] Although these two pairs differ only by the type of polycation, they exhibit very different assembly behavior in isolation, and when a multilayer of $(LPEI/PAA)_n$ is assembled atop $(PXV/PAA)_n$, the assembly of the heterostructure is disrupted. Here we investigate the nature of polyelectrolyte exchange that happens in these systems, demonstrating the true dynamic nature of the interdiffusion process, and its dependence on factors such as molecular weight. The driving force for polyion exchange in these systems is shown to be due to differences in the acid−base interactions between LPEI and PXV with PAA and a resulting difference in the degree of ionization of the polyacid. Inserting a blocking layer between the two multilayers prevented any disruption of the heterostructure and allowed straightforward heterostructure assembly, proving that disruption of this system results from LPEI interdiffusion. The applicability of this approach was further demonstrated in the construction of an LbL electrochromic device consisting of a coloring electrode and electrolyte. The use of blocking layers to manipulate growth modes in LbL assembled heterostructures[18,19] provides the precise control necessary to purposefully vary composition for true bottom-up assembly of complex devices. The added ability to isolate, or compartmentalize, portions of the LbL film may also lead to new applications.

Experimental Section[45]

Materials. Poly(hexylviologen) was synthesized by refluxing 4,4′-bipyridine and 1,6-dibromohexane (Sigma Aldrich) overnight in acetonitrile that had been dried over molecular sieves. The precipitate was then washed with acetonitrile and dried. Static light scattering (SLS) gave a weight-average molecular weight of 100 000 g/mol and end-group analysis via NMR gave a weight of 292 200 g/mol (see Supporting Information for details about the NMR analysis). Linear poly(ethylene imine), ≈25 and ≈250 kDa, and poly(acrylic acid), ≈90 kDa in 25 mass % aqueous solution, were purchased from Polysciences. Poly(allylamine hydrochloride) (PAH) was purchased from Sigma Aldrich. All chemicals were used as received. The chemical structures of these polyelectrolytes are shown in Figure 1.

Sample Preparation and Characterization. Film assembly was automated with a Carl Zeiss HMS DS-50 slide stainer. The substrates were exposed first to polycation solution for 10 min followed by three rinses in Milli-Q water and then a 10 min exposure to the polyanion solution followed again by rinsing. All polyelectrolyte solutions were 20 mM with respect to the polymer repeat unit. The pH of the polyelectrolyte solutions was adjusted with dilute aqueous solutions of HCl or NaOH; salt was not added to any polyelectrolyte solution. The pH of the rinse baths was adjusted to match that of the polyelectrolyte solutions; potassium phthalate buffer was used to adjust to pH 4, and HCl was used to adjust to pH 5.

Glass substrates were cleaned in a Bransonic ultrasonic cleaner for 15 min each in dichloromethane, acetone, methanol, and deionized water. The water cleaning was repeated twice. Immediately prior to film assembly the substrates were exposed to oxygen plasma for 5 min. Silicon substrates were ultrasonically cleaned first in a solution of 70% H_2SO_4 and 30% H_2O_2 and then a mixture of 50% NH_3OH 50% H_2O_2.

Thickness measurements were performed by ellipsometry and profilometry. A Gaertner single wavelength ellipsometer was used for films less than 100 nm thick. Ellipsometry was performed at a single incident angle of 70°, and the refractive index was fixed at 1.45. A Tencor P10 profilometer was used to measure thicker films, films which were not optically clear, and for all surface roughness measurements. A tip force of 3 mg was used to avoid penetrating the film. In all cases, films were dried in a nitrogen stream prior to measurement.

FTIR measurements were performed using a Nicolet Magna 860 Fourier transform infrared spectrometer with a DTGS detector. Films were assembled on silicon substrates, or assembled as free-standing films on poly(propylene) substrates as described elsewhere,[37] and examined in transmission mode.

Electrochemical potential control and current sensing were performed using an EG&G 263A potentiostat/galvanostat. Electrolyte was 0.1 M KCl, counter electrode was 2 cm^2 of platinum foil, and reference electrode was K-SCE. The three-electrode cell was constructed in a similar fashion to one previously described.[10]

Results and Discussion

Film Assembly. The design of our model heterostructure first required a study of the assembly of the two pairs of polyelectrolytes in isolation. PXV/PAA and LPEI/PAA films were assembled over a range of pH conditions atop the clean native oxide surfaces of silicon wafers to determine the assembly conditions for maximum film thickness. The pH of assembly controls the ionization density of the PAA and LPEI in solution, and therefore it should strongly influence the thickness, cross-link density, and morphology of the films that result.

Previous studies of LPEI/PAA films indicate a maximum thickness when assembled at pH 4.0−4.5.[24] This pH coincides with the pK_a of LPEI in solution, which is 4.0−5.0.[38−40] The pK_a of PAA in solution to ranges from about 5.5 to 6.5.[41−43] In our previous work, we proposed that the thickest films were observed in this pH regime because both polymers were only partially ionized, allowing for coiled or loopy deposition of both polyelectrolytes. The layer-by-layer deposition of weak polyelectrolytes or hydrogen-bonding systems in this weakly ionized pH regime often creates films with an individual layer pair thickness of 100 nm or greater, which is much thicker than LbL films formed from strong polyelectrolytes[24,28] and indeed thicker than the radius of gyration of the polyelectrolytes. This unusual behavior may result because weak polyelectrolytes can redistribute their ionization density to adopt lower energy configurations. Additional causes may include hydrogen-bonding and acid−base interactions, which do not occur in strong polyelectrolytes.[26,44]

We observed maximum film thickness to occur between pH 4 and 5, which is consistent with our previous work.[24] LPEI/PAA films exhibit average thicknesses of 70−90 nm per layer pair, with an rms roughness of 1−2 nm. Between pH 4 and pH

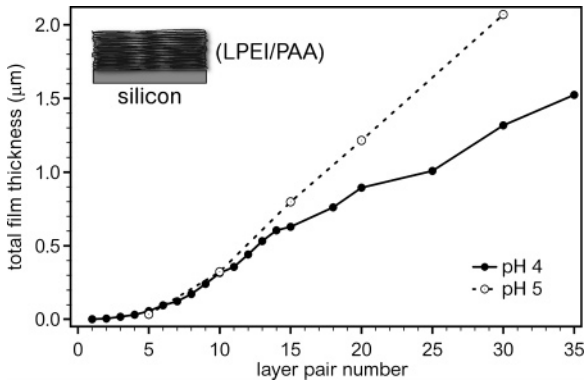

Figure 2. Growth curves for LPEI/PAA assembled at pH 4 and 5. A nonlinear growth regime is observed for the first 15 layer pairs, and then a linear, steady-state growth regime is reached. Standard uncertainty of film thickness measurement is ±10%.

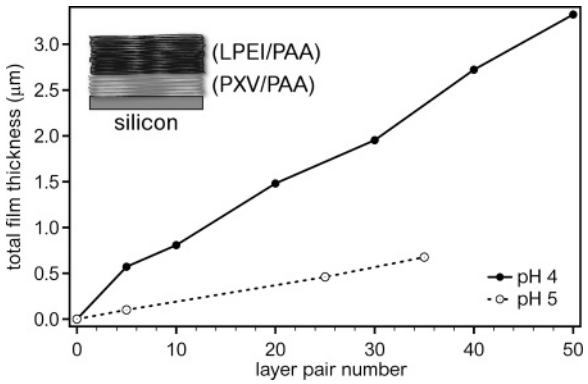

Figure 3. Growth curves for LPEI/PAA grown over PXV/PAA at pH 4 and pH 5, showing linear trends for both cases but with greater variance for the pH 4 case. Standard uncertainty of film thickness measurement is ±10%.

5 (and especially toward the lower end of this pH range) both polyelectrolytes are partially ionized. At pH lower than 2.5, when both LPEI and PAA are fully protonated, the per-layer pair thickness decreases and film formation is negligible. Film formation is also limited at pH values higher than 6, where PAA is fully ionized and therefore adsorbs in thin flat layers.

The increase of LPEI/PAA film thickness with layer pair number as shown in Figure 2 shows an initial regime of exponential-like growth, which lasts until around 15 layer pairs, after which growth becomes linear. While the phenomenon of early superlinear growth is universally reported for LbL assembled films, the superlinear regime is usually confined to the first 3−5 layer pairs.[23]

Films of $(PXV/PAA)_n$ were also assembled atop native silicon oxide over a similar pH range. Although PXV is not expected to change its ionization density with pH, the PXV solutions were adjusted to match the pH of the PAA solutions so that the polyanion would not change its ionization density during film assembly. The rms roughness of the $(PXV/PAA)_n$ films in the pH 4 and 5 cases is similar, averaging 8.1 and 12.1 nm, respectively. Growth is linear, with average per layer pair thicknesses of 55 nm for pH 4 and 60 for pH 5.

After the growth of the individual multilayers in isolation was studied, the model heterostructure was designed and assembled. Our original design consisted of a base electrochromic multilayer of $(PXV/PAA)_{20}$, followed by an ion conductive $(LPEI/PAA)_n$ multilayer, which was assembled at both pH 4 and pH 5. For simplicity, the $(PXV/PAA)_{20}$ multilayer was always assembled under the same pH conditions as the $(LPEI/PAA)_n$ multilayer. Figure 3 shows growth curves of the $(LPEI/PAA)_n$ multilayer assembled atop the base $(PXV/PAA)_{20}$ multilayer. The growth mode of the $(LPEI/PAA)_n$ multilayer atop the $(PXV/PAA)_{20}$ multilayer is similar to that of $(LPEI/PAA)_n$ in isolation atop the silicon oxide surface, in that it grows linearly over a large number of layer pairs. However, the pH 4 system grows to ≈90% of the thickness that it does on bare silicon oxide, while the pH 5 system grew to only ≈27% of the thickness on silicon oxide. The fact that the $(PXV/PAA)_{20}$ multilayers assembled at both pH 4 and pH 5 have similar surface roughness indicates that a changing substrate surface area did not cause the change in $(LPEI/PAA)_n$ growth.

Despite the similarity in growth mode and thickness, the model heterostructure assembled at pH 4 (shown in Figure 4) undergoes an extreme change in film morphology. The films become optically opaque after only a few layers of LPEI/PAA are assembled, indicating a roughness increase to several hundred nanometers or greater. Figure 4a shows that this change

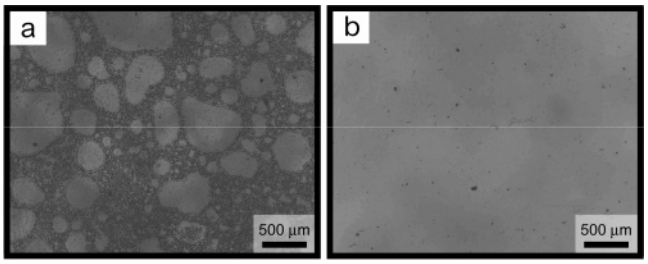

Figure 4. Surface of PXV/PAA + LPEI/PAA LbL film assembled at (a) pH 4, showing an uneven, roughened film surface, and (b) pH 5, showing a smooth film.

in opacity is accompanied by pitting on the heterostructure film surface. In contrast, when the $(LPEI/PAA)_n$ multilayer is assembled atop $(PXV/PAA)_n$ at pH 5, there is slightly increased opacity in the film, but no significant change in structure, as shown in Figure 4b.

FTIR Analysis. To probe the differences between $(LPEI/PAA)_n$ interactions and $(PXV/PAA)_n$ interactions, FTIR spectroscopy was used to measure the local chemical environment within the two systems assembled in isolation. Further FTIR spectroscopy experiments were used to observe the displacement of PXV by LPEI within the model heterostructure.

The degree of ionization along the backbone of a weak polyelectrolyte is known to vary from solution when within an LbL assembled film;[26] it depends strongly on the local environment of the polymer chain. Ionization distribution and ionization density along the polymer backbone are important factors in the stable formation of LbL films,[28] and weak polyelectrolytes may exhibit ionization redistribution to stabilize the resulting LbL film.[35,37] Several reports indicate that the carboxylic acid groups of PAA are more readily ionized in the presence of weak polycations.[26,27]

Figure 5 shows FTIR absorbance spectra for PAA cast from aqueous solution, PXV/PAA multilayers, and LPEI/PAA multilayers, assembled at both pH 4 and pH 5. Peaks at 1710 cm^{-1} correspond to −COOH asymmetric stretching, and those at about 1560 and 1400 cm^{-1} correspond to the $-COO^-$ asymmetric and symmetric stretches, respectively. The multilayer films exhibit more ionized (or bound) carboxylic acid groups than the cast PAA films exhibit.

The PXV/PAA and LPEI/PAA multilayers assembled at pH 4 exhibit a clear difference in the extent of PAA ionization. For PXV/PAA, the extent of ionization is 19.5%, whereas for LPEI/PAA the extent is 53%. For films assembled at pH 5, there is a smaller difference, with 38.5% PAA ionization in PXV/PAA and 54% in LPEI/PAA. For details as to how the

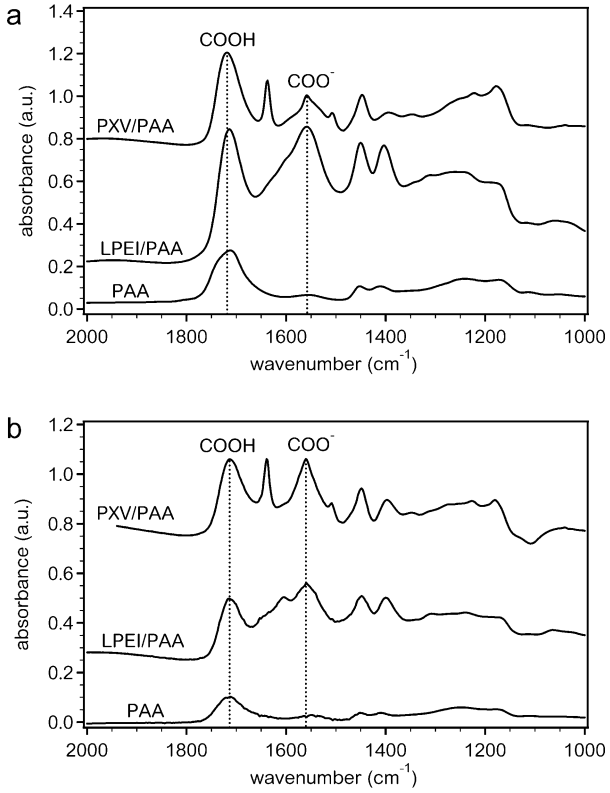

Figure 5. FTIR spectrum of cast PAA films, LPEI/PAA multilayers, and PXV/PAA multilayers assembled at (a) pH 4 and (b) pH 5. In all four films PAA becomes more ionized in respose to its environment, more so when complexed with LPEI than PXV. The difference in PAA ionization for the two systems is much greater at pH 4 than at pH 5. Spectra are vertically offset for clarity.

degree of ionization within the films was calculated, please see the Supporting Information. When assembled at pH 5, both systems have a relatively similar proportion of ionic cross-links. At pH 4, LPEI/PAA is a more ionically cross-linked complex.

This result suggests a mechanism for the destabilization of the PXV/PAA multilayer within the model heterostructure. The formation of ionic cross-links is energetically favored, and LPEI promotes more ionic cross-links. LPEI appears to "titrate" PAA so that it becomes more ionized and capable of forming additional electrostatic cross-links. Therefore, the spatial displacement of PXV by LPEI within the first multilayer is energetically favored. The wholesale rearrangement of film structure that accompanies this displacement may be responsible for the dramatic roughening of the film surface and the formation of pits. At pH 5, PAA ionization is more similar for the $(LPEI/PAA)_n$ and $(PXV/PAA)_n$ systems, and the driving force for PXV displacement is smaller, leading to slower film destabilization.

The displacement mechanism for model heterostructure destabilization can be confirmed by exposing the base $(PXV/PAA)_n$ multilayer to LPEI solution and monitoring the film composition over time. Similar experiments have been used to probe the relative strength of the interactions between polyelectrolytes within an LbL assembly.[32] Figure 6 shows the compositional progression of $(PXV/PAA)_{25}$ films immersed in various solutions of LPEI. Over time several changes can be observed in the FTIR spectra of the immersed films. A peak at 1640 cm^{-1}, which corresponds to C═C stretching, decreases, whereas a secondary amine peak ($-NH^{2+}$) at 1610 cm^{-1} becomes present and grows as the extent of PAA ionization increases. Also, a peak at 1400 cm^{-1}, which corresponds to the C−H deformation vibrations of the backbone of LPEI (corresponds to stretching of the C−H bonds of carbon singly bonded to nitrogen), grows as the exchange takes place. This change in composition clearly illustrates the interdiffusion of LPEI into the PXV/PAA bulk, the displacement of PXV with LPEI, and the corresponding increase in electrostatic cross-linking involving PAA. For 25 kDa LPEI solution at pH 4, the C═C peak completely disappeared after 12 h, and the percentage of ionized carboxyl groups increased from 18% to 60%. For immersion in 250 kDa LPEI solution, the same replacement occurs but at a slower rate. After 2 days in the 250 kDa LPEI solution, C═C remains, and the ratio of ionized to neutral carboxyl groups changed from 19% to 44%, indicating incomplete exchange. Immersion in pH 5 25 kDa LPEI solution creates a similar trend; disappearance of the C═C peak occurs as well as an increased ionization of carboxyl groups, but at a slower rate than immersion in pH 4 solution. These results confirm that LPEI is the diffusing species within the multilayer (if it was PAA, the molecular weight of the LPEI should not change the time for the process to occur) and that the driving force for this exchange process is stronger at pH 4 than at pH 5.

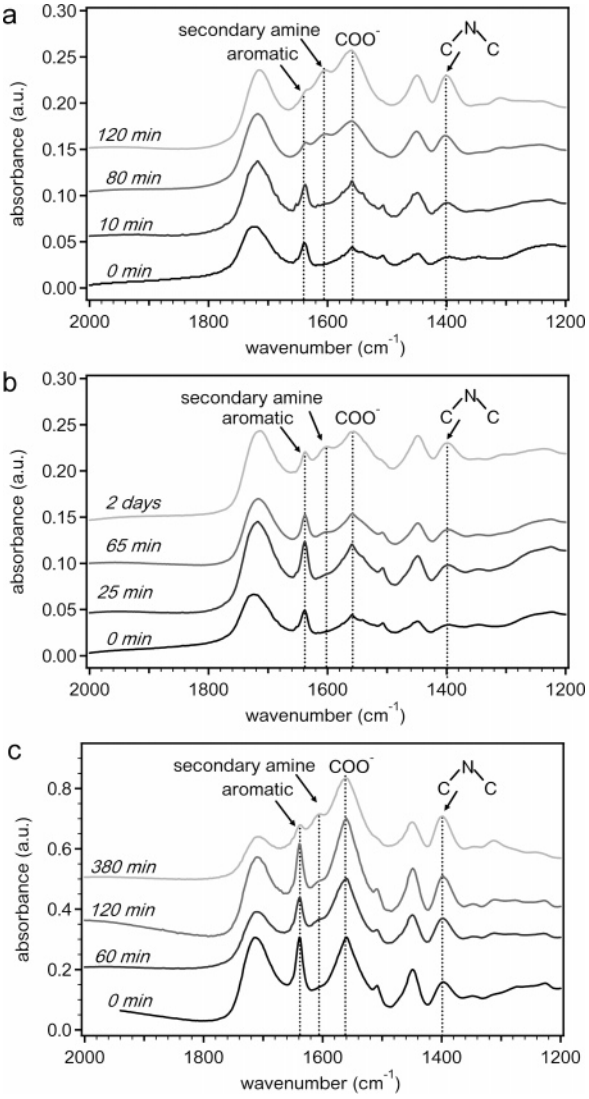

Figure 6. FTIR spectrum showing progression of LPEI exchanging with PXV at (a) 25 kDa LPEI at pH 4, (b) 250 kDa LPEI at pH 4, and (c) 25 kDa LPEI at pH 5. Exchange occurs in all three cases, most quickly at pH 4 for the 25 kDa LPEI, showing both that the process is diffusion limited and that the driving force for exchange is less at pH 5. Spectra are vertically offset for clarity.

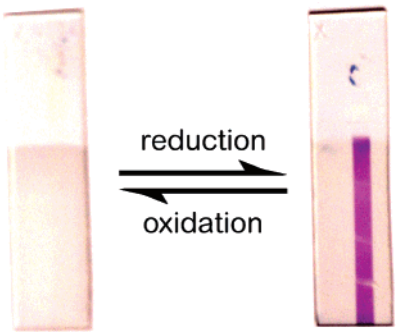

Figure 7. Redox switching of heterostructured film with cross-linked layers, indicating that PXV has not been displaced and that small ion motion has not been hindered by the cross-linked barrier layers.

Film Compartmentalization. The complex interactions within our model heterostructure clearly do not allow its straightforward bottom-up assembly. LPEI from the ion conduction multilayer diffuses into the electrochromic PXV/PAA multilayer, it exchanges with and displaces PXV, and it changes the electrostatic cross-link density, leading to a dramatic decrease in film quality. To prevent this disruption, a blocking layer strategy was employed. In this strategy, layers of a third system—$(PAH/PAA)_n$—were assembled in between the electrochromic PXV/PAA multilayer and the ion conductive LPEI/PAA multilayer. After the PXV/PAA base layer was assembled, four layers of PAH/PAA were assembled on top of the film. The film was then heated at 130 °C for 1.5 h to form covalent cross-links between the carboxyl and amine groups in PAA/PAH.[22] Elsewhere, similar blocking layers have been reported[18,19] as well as strategies to compartmentalize multilayers by using clay platelets.[20−22] After covalent cross-link formation, the LPEI/PAA multilayer was assembled onto the film. The resultant heterostructured film was optically clear, and its rms roughness was only 1 nm. The heterostructure with the blocking layers is about 3.5 μm thick or 30% thinner than the heterostructure assembled without blocking layers, which is about 5.0 μm thick; LPEI/PAA assembled onto the blocking layer grows at the same linear rate as in isolation atop native silicon oxide, with 30 bilayers assembled at pH 4 measuring ~1.3 μm. The PAH/PAA film is too thin to allow for LPEI to diffuse into it, and the PAH chains are extended at this pH, making the PAH/PAA layers even less permeable.

Heating an LbL assembled film can smooth the film surface. To determine whether the increase in the heterostructure film stability was due to the covalently cross-linked blocking layer or the simple effect of heat, the PXV/PAA base multilayer was assembled and then heated at 130 °C for 1.5 h, after which an LPEI/PAA multilayer was assembled onto the film. The heterostructure assembly was still disrupted; the film was optically opaque, and its rms roughness was 10 nm. Although simple heating did reduce the roughness of the heterostructure film, it did not provide the control over stability that is afforded by the blocking layer strategy.

To demonstrate that the blocking layer strategy prevents PXV displacement, we constructed our model heterostructure with a blocking layer atop an ITO substrate. The functional model heterostructure atop ITO was employed as the working electrode in an electrochemical cell as described elsewhere in our work,[10] and photographs were recorded of the electrochromism of PXV, as shown in Figure 7. The clear change in color from transparent to purple indicates that the underlying PXV/PAA layers are intact. The switching speed of the functional heterostructure is not measurably slowed by the presence of the blocking layer (compared to a PXV/PAA film assembled in isolation), indicating that the blocking layer does not impede small ion motion. The high ion conductivity of the thick LPEI/PAA multilayer also apparently avoids any negative impact on switching speed. This demonstration clearly shows that *working* functional heterostructures may be constructed by layer-by-layer assembly using a blocking layer strategy. Implementing this strategy eliminates the standing technical barriers to the creation of complex thin film devices containing three or more functional multilayers.

Conclusions

The formation of functional heterostructured thin films by LbL assembly is often disrupted by complex interactions between polyelectrolytes. The mobility of polymer chains through the film is responsible for some types of heterostructure disruption, and the wholesale rejection of some heterostructure components is a possible outcome. This phenomenon shares its mechanism with the superlinear growth mode that is observed in some LbL assembled systems. In the early stages of its development, LbL assembly was regarded as a surface modification technique, where the bulk film was considered to be a glassy, inert solid. This perspective should be reexamined because in many cases the entire film participates in the assembly process.

The disrupted assembly of our electrochrome/electrolyte system results from an exchange/displacement mechanism. The polymer being displaced was of high MW, showing that the exchange process was driven not by the entropic gain from releasing oligimeric molecules but rather the differences in the strength of interaction of PXV and PAA and LPEI and PAA. Through FTIR spectroscopy we observed that LPEI from the ion conducting multilayer diffuses into the bulk of the electrochromic $(PXV/PAA)_n$ multilayer below it, exchanging with and eventually displacing PXV. We hypothesize that displacement occurs because PAA prefers interactions with LPEI over PXV. The ionization density of PAA is far greater when it is paired with LPEI than when it is paired with PXV. The ability of LPEI to "titrate" PAA and form additional electrostatic cross-links with unpaired carboxylic acids in the bulk film may be related to the superlinear growth of the $(LPEI/PAA)_n$ system in isolation. The system grows superlinearly for more than 15 layer pairs before it reaches a linear growth regime; typical LbL assembled systems only grow superlinearly for three layer pairs.[23] This clear correlation between superlinear growth and atypical heterostructure assembly behavior illustrates that these two phenomena share the same underlying interdiffusion mechanism. Simple and effective strategies to overcome assembly disruption, such as the blocking layer used here, become obvious only after the mechanism of this disruption is understood.

Acknowledgment. This work made use of the Shared Experimental Facilities at MIT's Center for Materials Science and Engineering supported in part by the MRSEC program of the National Science Foundation under Award DMR 02-13282. This research was supported in part by the U.S. Army through the Institute for Soldier Nanotechnologies, under Contract DAAD-19-02-D-0002 with the U.S. Army Research Office. The content does not necessarily reflect the position of the government, and no official endorsement should be inferred.

Supporting Information Available: Experimental details. This material is available free of charge via the Internet at http://pubs.acs.org.

References and Notes

(1) Decher, G.; Schlenoff, J. B. *Multilayer Thin Films: Sequential Assembly of Nanocomposite Materials*; Wiley-VCH: Weinheim, 2003.
(2) Hammond, P. T. *Adv. Mater.* **2004**, *16*, 1271−1293.
(3) Xie, A. F.; Granick, S. *Macromolecules* **2002**, *35*, 1805−1813.
(4) Mermut, O.; Barrett, C. J. *J. Phys. Chem. B* **2003**, *107*, 2525−2530.
(5) Hübsch, E.; Fleith, G.; Fatisson, J.; Labbé, Voegel, J. C.; Schaaf, P.; Ball, V. *Langmuir* **2005**, *21*, 3664−3669.
(6) Korneev, D.; Lvov, Y.; Decher, G.; Schmitt, J.; Yaradaikin, S. *Physica B* **1995**, *213/214*, 954.
(7) Kellogg, G. J.; Mayes, A. M.; Stockton, W. B.; Ferreira, M.; Rubner, M. F.; Satija, S. K. *Langmuir* **1996**, *12*, 5109−5113.
(8) Arys, X.; Laschewsky, A.; Jonas, A. M. *Macromolecules* **2001**, *34*, 3318−3330.
(9) Shiratorei, S. S.; Rubner, M. F. *Macromolecules* **1998**, *31*, 4309−4318.
(10) DeLongchamp, D. M.; Kastantin, M.; Hammond, P. T. *Chem. Mater.* **2003**, *15*, 1575−1586.
(11) Schoeler, B.; Poptoshev, E.; Caruso, F. *Macromolecules* **2003**, *36*, 5258−5264.
(12) Lavalle, P.; Gergely, C.; Cuisinier, F. J. G.; Decher, G.; Schaaf, P.; Voegel, J. C. *Macromolecules* **2002**, *35*, 4458−4465.
(13) Lavalle, P.; Picart, C.; Mutterer, J.; Gergely, C.; Reiss, H.; Voegel, J. C.; Senger, B.; Schaaf, P. *J. Phys. Chem. B* **2004**, *108*, 635−648.
(14) Hübsch, E.; Ball, V.; Senger, B.; Decher, G.; Voegel, J. C.; Schaaf, P. *Langmuir* **2004**, *20*, 1980−1985.
(15) Lavalle, P.; Vivet, V.; Jessel, N.; Decher, G.; Voegel, J. C.; Mesini, P.; Schaaf, P. *Macromolecules* **2004**, *37*, 1159−1162.
(16) Yoo, P. J.; Nam, K.; Qi, J.; Lee, S.; Park, J.; Belcher, A.; Hammond, P. T. *Nat. Mater.* **2006**, *5*, 234−240.
(17) Jomaa, H. W.; Schlenoff, J. B. *Langmuir* **2005**, *21*, 8081−8084.
(18) Garza, J. M.; Schaaf, P.; Muller, S.; Ball, V.; Stolz, J. F.; Voegel, J. C.; Lavalle, P. *Langmuir* **2004**, *20*, 7298−7302.
(19) Wood, K. C.; Chuang, H. F.; Batten, R. D.; Lynn, D. M.; Hammond, P. T. *Proc. Natl. Acad. Sci. U.S.A.* **2006**, *103*, 10207−10212.
(20) Glinel, K.; Laschewsky, A.; Jonas, A. M. *Macromolecules* **2001**, *34*, 5267−5274.
(21) Struth, B.; Eckle, M.; Decher, G.; Oeser, R.; Simon, P.; Schubert, D. W.; Schmitt, J. *Eur. Phys. J. E* **2001**, *6*, 351−358.
(22) Vuillaume, P. Y.; Glinel, K.; Jonas, Am. M.; Laschesky, A.
(23) Ladam, G.; Schaad, P.; Voegel, J. C.; Schaaf, P.; Decher, G.; Cuisinier, F. *Langmuir* **2000**, *16*, 1249−1255.
(24) DeLongchamp, D. M.; Hammond, P. T. *Chem. Mater.* **2003**, *15*, 1165−1173.
(25) Harris, J. J.; DeRose, P. M.; Bruening, M. L. *J. Am. Chem. Soc.* **1999**, *121*, 1978−1979.
(26) Choi, J.; Rubner, M. F. *Macromolecules* **2005**, *38*, 116−124.
(27) Kharlampieva, E.; Sukishvili, S. A. *Lamgmuir* **2003**, *19*, 1235−1243.
(28) Sukishvili, S. A.; Granick, S. *Macromolecules* **2002**, *35*, 301−310.
(29) Voight, U.; Khrenov, V.; Thuer, K.; Hahn, M.; Jaeger, W.; von Klitzing, R. *J. Phys.: Condens. Matter* **2003**, *15*, S213−S218.
(30) Kolarik, L.; Furlong, D. N.; Joy, H.; Struijk, C.; Rowe, R. *Langmuir* **1999**, *15*, 8265−8275.
(31) Ball, V.; Hübsch, E.; Schweiss, R.; Voegel, J. C.; Schaaf, P.; Knoll, W. *Langmuir* **2005**, *21*, 8526−8531.
(32) Schoeler, B.; Poptoshev, E.; Caruso, F. *Macromolecules* **2003**, *36*, 5258−5264.
(33) Quinn, J. F.; Yeo, J. C. C.; Caruso, F. *Macromolecules* **2004**, *37*, 6537−6543.
(34) Debreczeny, M.; Ball, V.; Boulmedais, F.; Szalontat, B.; Voegel, J. C.; Schaaf, P. *J. Phys. Chem. B* **2003**, *107*, 12734−12739.
(35) Johal, M. S.; Ozer, B. H.; Casson, J. L.; St. John, A.; Robinson, J. M.; Wang, H. L. *Langmuir* **2004**, *20*, 2792−2796.
(36) Sukhishvili, S. A.; Granick, S. *Langmuir* **2003**, *19*, 1980−1983.
(37) Lutkenhaus, J. L.; Hrabak, K. D.; McEnnis, K.; Hammond, P. T. *J. Am. Chem. Soc.* **2005**, *127*, 17228−17234.
(38) Bloys van Treslong, C. J. *Recl.: J. R. Neth. Chem. Soc.* **1978**, *97*, 13−21.
(39) Weyts, K. F.; Goethals, E. J. *Makromol. Chem., Rapid Commun.* **1989**, *10*, 299−302.
(40) Smits, R. G.; Koper, G. J. M.; Mandel, M. *J. Phys. Chem.* **1993**, *97*, 5745−5751.
(41) Bromberg, L. *J. Phys. Chem. B* **1998**, *102*, 10736−10744.
(42) Philippova, O. E.; Hourdet, D.; Andebert, R.; Khokhlov, A. R. *Macromolecules* **1997**, *30*, 8278−8285.
(43) Petrov, A. I.; Antipov, A. A.; Sukhorukov, G. B. *Macromolecules* **2003**, *36*, 10079−10086.
(44) Burke, S. E.; Barrett, C. J. *Langmuir* **2003**, *19*, 3297−3303.

(45) Certain equipment, instruments, or materials are identified in this paper in order to adequately specify the experimental details. Such identification does not imply recommendation by the National Institute of Standards and Technology nor does it imply the materials are necessarily the best available for the purpose.

MA061080F